Electronic Supplementary Material (ESI) for Inorganic Chemistry Frontiers.


**Supporting information**

# Spinel structured metal oxide embedded MXene nanocomposites for efficient water splitting reactions

Dhanasekaran Vikraman[a], Sajjad Hussain[b,c], Liu Hailiang[d], K. Karuppasamy[a], Periyasamy Sivakumar[e], P. Santhoshkumar[f], Jongwan Jung[b,c], Hyun-Seok Kim[a*]

[a.]Division of Electronics and Electrical Engineering, Dongguk University-Seoul, Seoul 04620, Korea.
[b.]Department of Nanotechnology and Advanced Materials Engineering, Sejong University, Seoul 05006, Korea.
[c.]Hybrid Materials Center (HMC), Sejong University, Seoul 05006, Korea.
[d.]Convergence Semiconductor Research Center, Department of Electronics and Electrical Engineering, Dankook University, Yongin 16890, Korea.
[e.]Advanced Functional Nanohybrid Material Laboratory, Department of Chemistry, Dongguk University-Seoul, Seoul 04620, Korea.
[f.]Millimeter-wave Innovation Technology (MINT) Research Centre, Dongguk University-Seoul, Seoul 04620, Korea.

*Email: hyunseokk@dongguk.edu; Tel: +82-2-2260-3996; Fax: +82-2-2277-8735

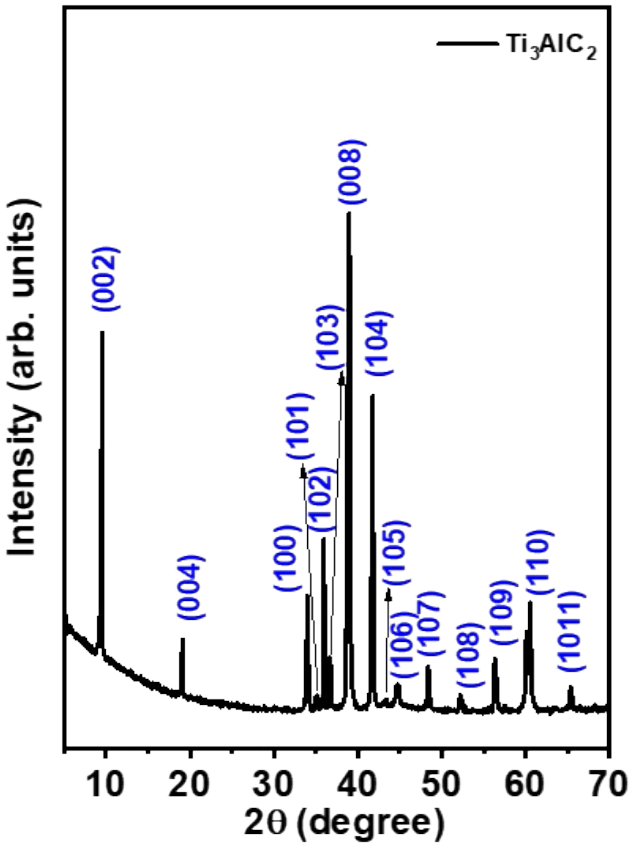


**Figure S1.** XRD pattern of MAX phase $Ti_3AlC_2$.

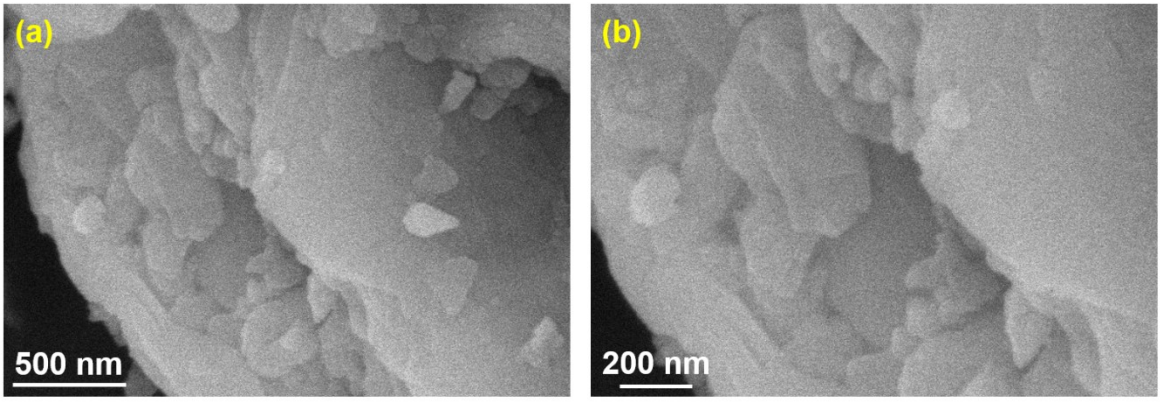


**Figure S2**. FESEM images of MAX phase with different magnifications

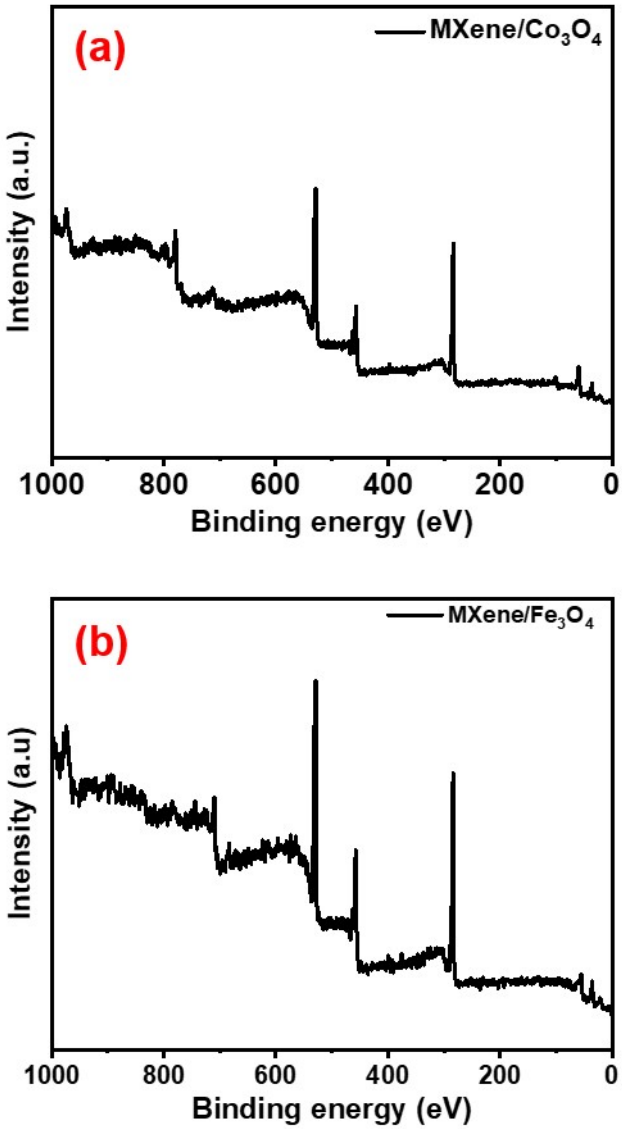


**Figure S3.** XPS survey spectra for the (a) MXene/$Co_3O_4$ and (b) MXene/$Fe_3O_4$ nanocomposites.

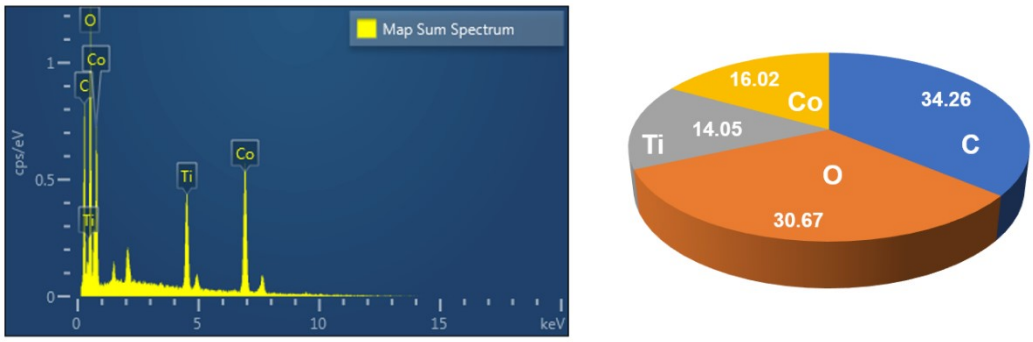


**Figure S4.** EDX spectrum and their composition chart for MXene/$Co_3O_4$ nanocomposites

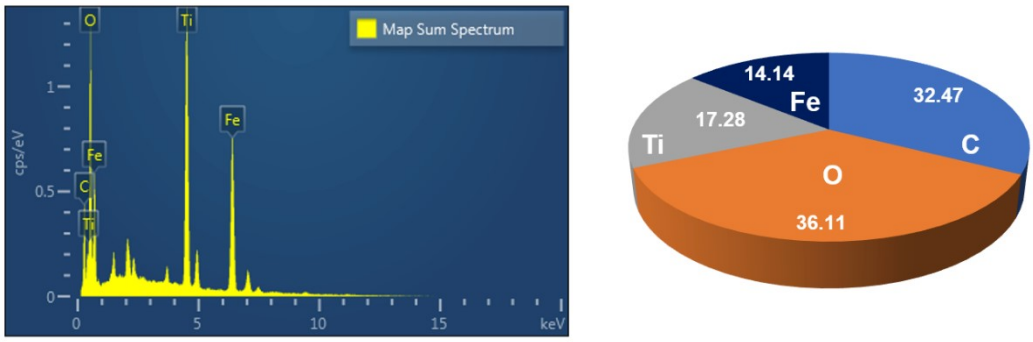


**Figure S5.** EDX spectrum and their composition chart for MXene/$Fe_3O_4$ nanocomposites

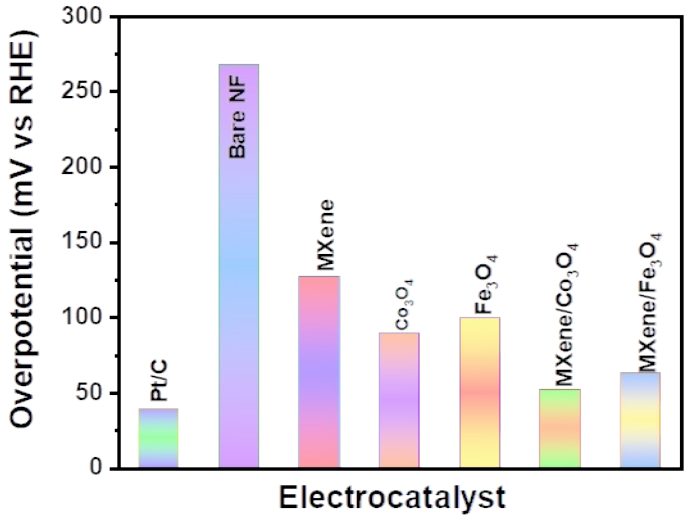


**Figure S6.** HER overpotential for bare NF, Pt/C, MXene, $Co_3O_4$, $Fe_3O_4$, MXene/$Co_3O_4$, and MXene/$Fe_3O_4$ composites

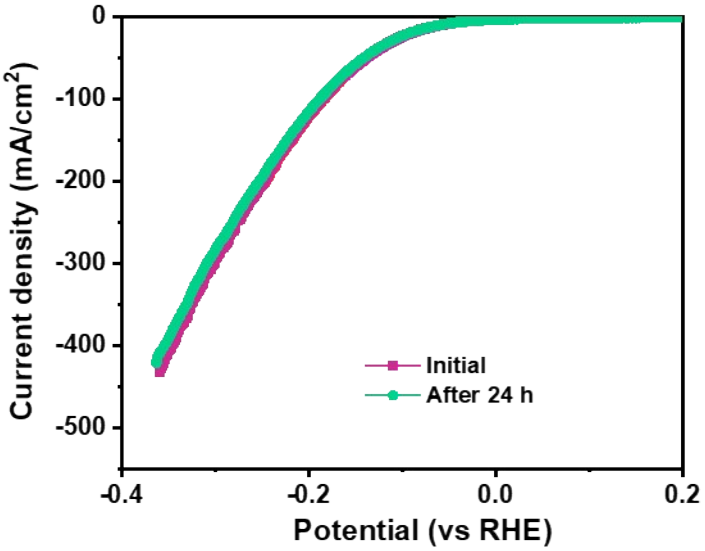


**Figure S7.** LSV profiles before and after 24 h continuous OER reaction

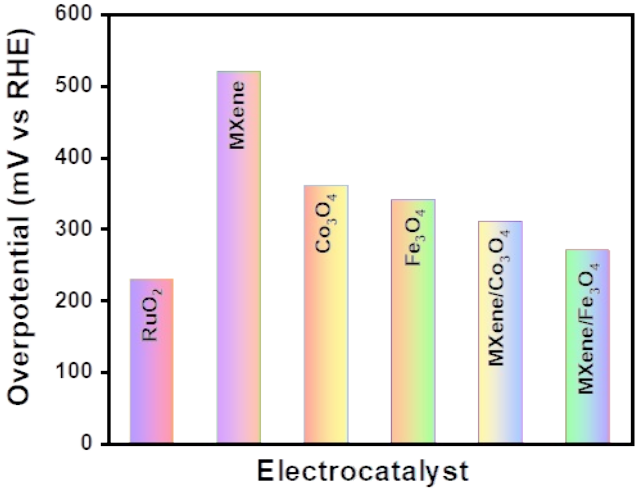


**Figure S8.** OER overpotential for $RuO_2$, MXene, $Co_3O_4$, $Fe_3O_4$, MXene/$Co_3O_4$, and MXene/$Fe_3O_4$ composites

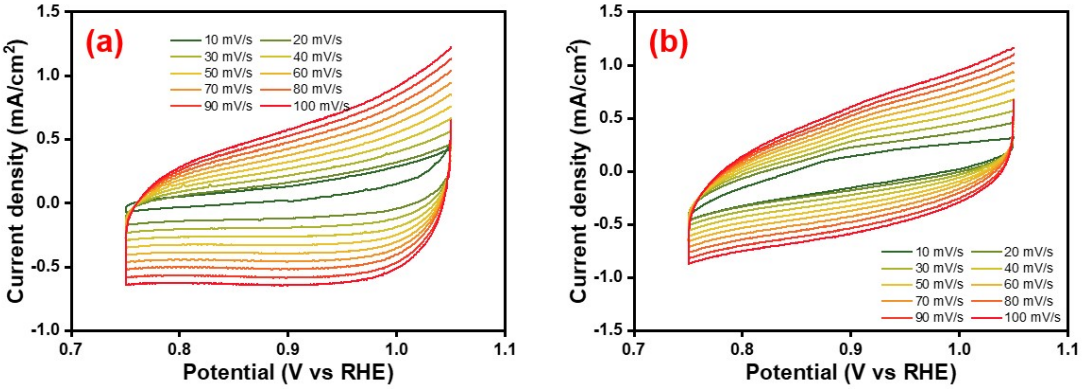


**Figure S9.** Non-faradaic region CVs for the(a) MXene/$Co_3O_4$ and (b) MXene/$Fe_3O_4$ nanocomposites at different scan rates.

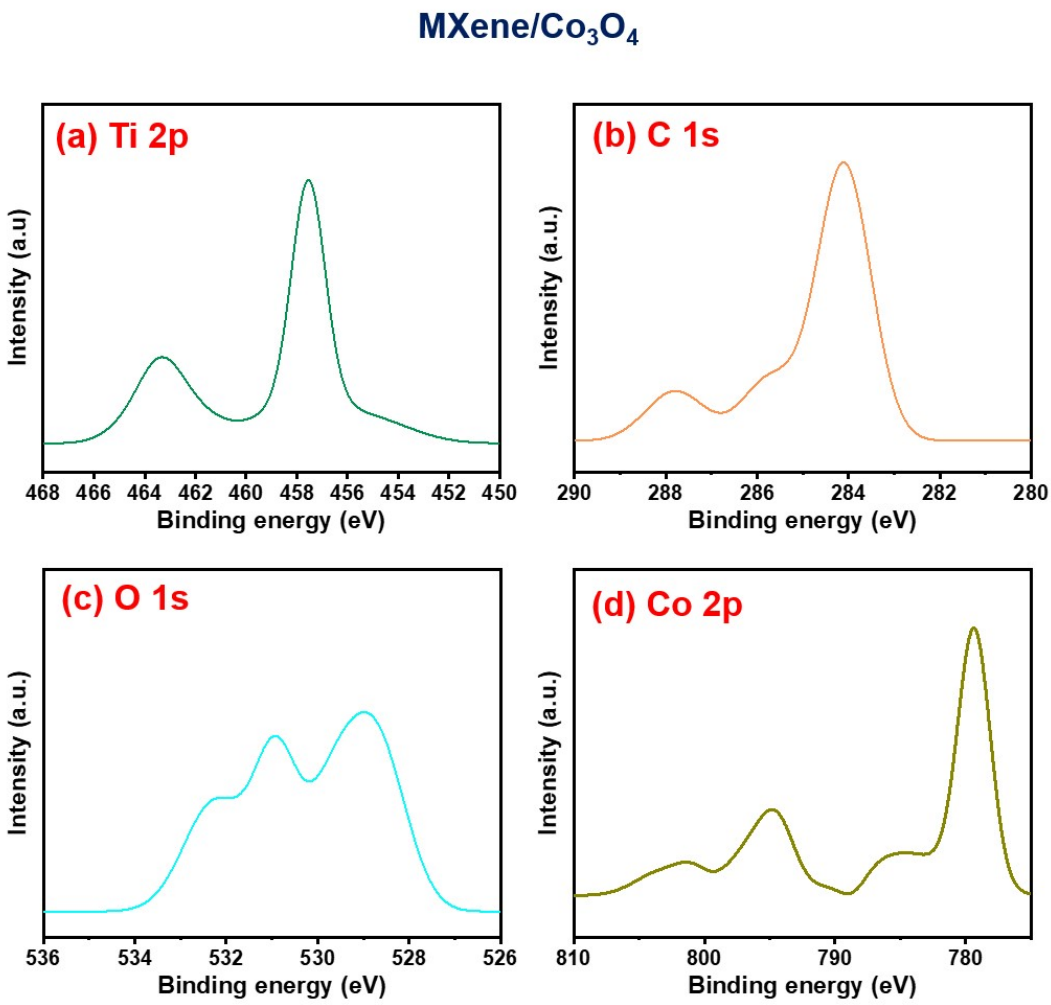


**Figure S10.** XPS profiles after 24 h overall water splitting for MXene/$Co_3O_4$ composites: (a) Ti 2p, (b) C 1s, (h) O 1s and (d) Co 2p regions

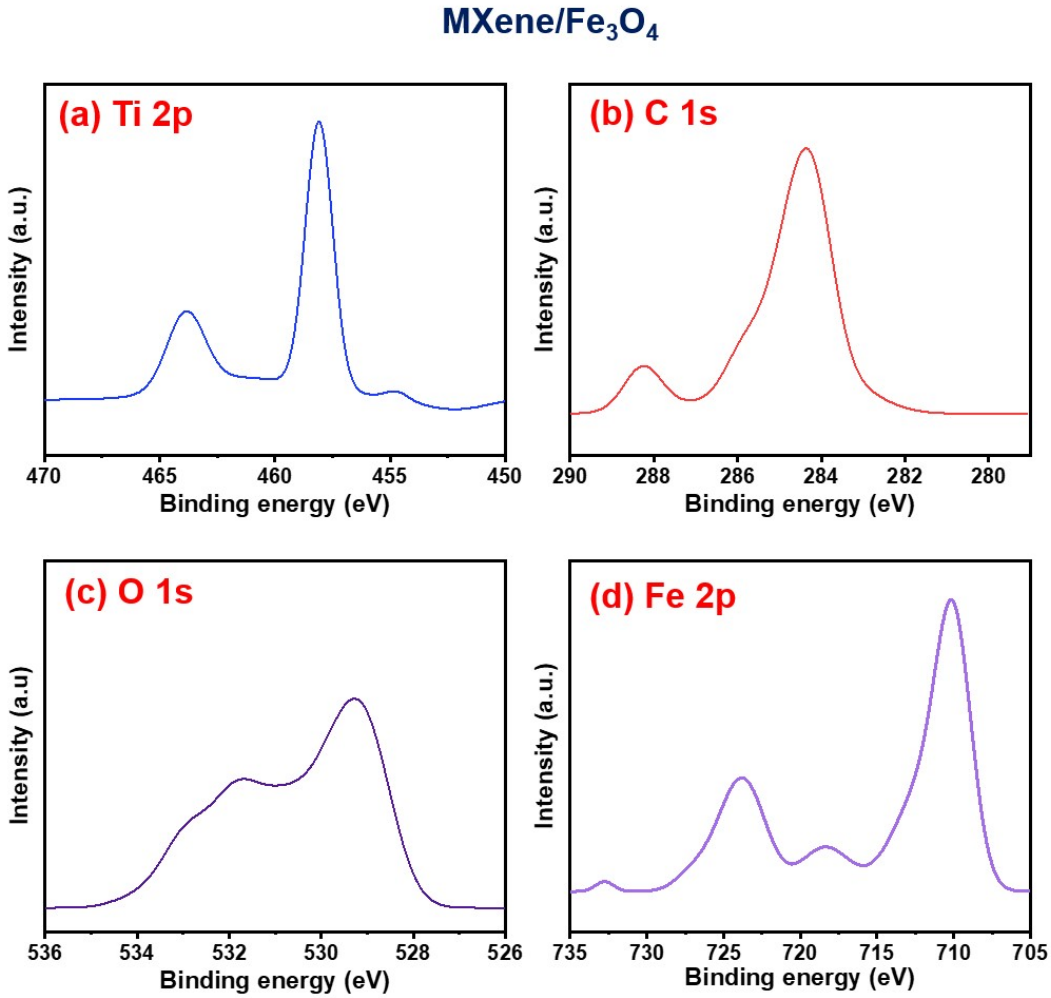


**Figure S11.** XPS profiles after 24 h overall water splitting for MXene/$Fe_3O_4$ composites: (a) Ti 2p, (b) C 1s, (h) O 1s and (d) Fe 2p regions

**Table S1.** $N_2$ sorption analysis of metal oxide, MXene and their composites.

| **Sample** | **BET ($m^2.g^{-1}$)** | **Pore volume ($cm^3.g^{-1}$)** | **Mean pore diameter (nm)** |
|---|---|---|---|
| MXene | 4.67 | 0.041 | 35.41 |
| $Co_3O_4$ | 6.23 | 0.035 | 22.45 |
| $Fe_3O_4$ | 3.42 | 0.024 | 27.56 |
| MXene/$Co_3O_4$ | 13.3 | 0.076 | 22.91 |
| MXene/$Fe_3O_4$ | 9.06 | 0.052 | 22.93 |

**Table S2.** HER catalytic performances MXene@oxide-based electrocatalysts

| Electrocatalyst | Electrolyte | η (mV) | Tafel Slope ($mV \cdot dec^{-1}$) | Ref. |
|---|---|---|---|---|
| MXene/$Co_3O_4$ | 1 M KOH | 52 @ 10 $mA/cm^2$ | 59 | This work |
| MXene/$Fe_3O_4$ | 1 M KOH | 62 @ 10 $mA/cm^2$ | 81 | |
| FeNi@MXene ($Mo_2TiC_2T_x$) | 1M KOH | 160@ 10 $mA/cm^2$ | 103.46 | [1] |
| $MoS_2$@$Mo_2CTx$ | 0.5M $H_2SO_4$ | 176@10 mA/cm | 207 | [2] |
| $Mo_2CT_x$/2H-$MoS_2$ nanohybrid | 0.5M $H_2SO_4$ | 119@10 mA/cm | 60 | [3] |
| Co-CoO/$Ti_3C_2$- MXene/NF | 1M KOH | 45@10 mA/cm | 47 | [4] |
| Pd@$MoS_2$/$Mo_2TiC_2T_x$ | 0.5M $H_2SO_4$ &1M KOH | 92 and 100 @10 mA/cm | 60 & 80 | [5] |
| MWCNT/$V_2CTx$ | 1M KOH | 27@ 10 $mA/cm^2$ | 41 | [6] |
| $FeS_2$@MXene | 1M KOH | 87@ 10 $mA/cm^2$ | 97.7 | [7] |
| $Mo_2C$/graphene | 0.5M $H_2SO_4$ | 236@10 mA/cm | 73 | [8] |
| $Mo_2CTx$:Co | 0.5M $H_2SO_4$ | 180@10 mA/cm | 59 | [9] |
| Defect-rich $CoS_{1.097}$/$MoS_2$ | 0.5M $H_2SO_4$, 1M KOH & 1M PBS | 228, 249 & 341@10 mA/cm | 59, 75 and 85 | [10] |
| $NiFe_2O_4$/$Ti_3C_2$ | 1M KOH | 173@ 10 $mA/cm^2$ | 112.2 | [11] |
| $CoS_2$@MXene | 1M KOH | 175@ 10 $mA/cm^2$ | 97 | [12] |
| $Co(S_xSe_{1-x})_2$ | 1M KOH | 122@ 10 $mA/cm^2$ | 86 | [13] |
| $Ni_{0.9}Fe_{0.1}PS_3$@ MXene | 1M KOH | 198@ 10 $mA/cm^2$ | 114 | [14] |
| CoP@MXene | 1M KOH | 116@ 10 $mA/cm^2$ | 57 | [15] |
| Ni/NiS/NC | 1M KOH | 70@ 10 $mA/cm^2$ | 45 | [16] |
| Mesh CrFe-CoP NSs | 1M KOH | 103.7@ 10 $mA/cm^2$ | 90.9 | [17] |
| Co-$Ni_xP_y$@$Co_3O_4$ | 1M KOH | 72@ 10 $mA/cm^2$ | - | [18] |
| Ru-SA/$Ti_3C_2T_x$ | 1M KOH | 70@ 10 $mA/cm^2$ | 27.7 | [19] |

**Table S3.** OER catalytic performances MXene@oxide-based electrocatalysts

| Electrocatalyst | Electrolyte | η (mV) | Tafel Slope ($mV \cdot dec^{-1}$) | Ref. |
|---|---|---|---|---|
| MXene/$Co_3O_4$ | 1 M KOH | 310@ 10 $mA/cm^2$ | 74 | This work |
| MXene/$Fe_3O_4$ | 1 M KOH | 270 @ 10 $mA/cm^2$ | 54 | |
| FeNi@MXene ($Mo_2TiC_2T_x$) | 1M KOH | 190@ 10 $mA/cm^2$ | 42.78 | [1] |
| $Fe_3O_4/Ti_3C_2T_x$ | 1M KOH | 290@ 10 $mA/cm^2$ | 65.1 | [20] |
| $Co_3O_4/Ti_3C_2T_x$ | 1M KOH | 300 mV@ 10 $mA/cm^2$ | 118 | [21] |
| Co-CoO/$Ti_3C_2$- MXene/NF | 1M KOH | 271@10 mA/cm | 47 | [4] |
| MWCNT/$V_2CTx$ | 1M KOH | 469@ 10 $mA/cm^2$ | 77 | [6] |
| $FeS_2$@MXene | 1M KOH | 240@ 10 $mA/cm^2$ | 58.7 | [7] |
| $NiFe_2O_4/Ti_3C_2$ | 1M KOH | 266@ 10 $mA/cm^2$ | 73.6 | [11] |
| $CoS_2$@MXene | 1M KOH | 150@ 10 $mA/cm^2$ | 92 | [12] |
| $Co(S_xSe_{1-x})_2$ | 1M KOH | 151@ 10 $mA/cm^2$ | 65.5 | [13] |
| $Ni_{0.9}Fe_{0.1}PS_3$@ MXene | 1M KOH | 152@ 10 $mA/cm^2$ | 36.5 | [14] |
| CoP@MXene | 1M KOH | 146@ 10 $mA/cm^2$ | 32.5 | [15] |
| $NiCoS/Ti_3C_2T_x$ | 1M KOH | 365@ 10 $mA/cm^2$ | 58 | [22] |
| Ni/NiS/NC | 1M KOH | 337@ 10 $mA/cm^2$ | 52 | [16] |
| Mesh CrFe-CoP NSs | 1M KOH | 256.4@ 10 $mA/cm^2$ | 55.9 | [17] |
| Co-$Ni_xP_y$@$Co_3O_4$ | 1M KOH | 120@ 10 $mA/cm^2$ | - | [18] |
| IrCo@ac-$Ti_3C_2$ | 1M KOH | 220@ 10 $mA/cm^2$ | 60 | [23] |
| Ru-SA/$Ti_3C_2T_x$ | 1M KOH | 290@ 10 $mA/cm^2$ | 37.9 | [19] |
| $Ni_{0.7}Fe_{0.3}PS_3$@$Ti_3C_2T_m$ | 1M KOH | 282@ 10 $mA/cm^2$ | 36.5 | [14] |

**Table S4.** Comparison of overall water splitting of MXene@oxide with various electrocatalysts.

| Electrocatalyst | Electrolyte | Cell voltage (V) | Ref. |
|---|---|---|---|
| MXene/$Co_3O_4$ | 1 M KOH | 1.51 @ 10 mA/cm$^2$ | This work |
| MXene/$Fe_3O_4$ | 1 M KOH | 1.54 @ 10 mA/cm$^2$ | |
| FeNi@MXene ($Mo_2TiC_2T_x$) | 1M KOH | 1.74 @ 50 mA/cm$^2$ | [1] |
| Co-CoO/$Ti_3C_2$ | 1M KOH | 1.55 @10 mA/cm$^2$ | [4] |
| $FeS_2$@MXene | 1M KOH | 1.57 @ 10 mA/cm$^2$ | [7] |
| $CoS_2$@MXene | 1M KOH | 1.62 @ 10 mA/cm$^2$ | [12] |
| $Co(S_xSe_{1-x})_2$ | 1M KOH | 1.63 @ 10 mA/cm$^2$ | [13] |
| $Ni_{0.9}Fe_{0.1}PS_3$@ MXene | 1M KOH | 1.65 @ 10 mA/cm$^2$ | [14] |
| CoP@MXene | 1M KOH | 1.56 @ 10 mA/cm$^2$ | [15] |
| Ni/NiS/NC | 1M KOH | 1.61 @ 10 mA/cm$^2$ | [16] |
| Mesh CrFe-CoP NSs | 1M KOH | 1.55 @ 10 mA/cm$^2$ | [17] |
| Co-$Ni_xP_y$@$Co_3O_4$ | 1M KOH | 1.47 @ 10 mA/cm$^2$ | [18] |
| Ru-SA/$Ti_3C_2T_x$ | 1M KOH | 1.56 @ 10 mA/cm$^2$ | [19] |

**References**

[1] J. Wang, P. He, Y. Shen, L. Dai, Z. Li, Y. Wu, C. An, FeNi nanoparticles on Mo2TiC2Tx MXene@ nickel foam as robust electrocatalysts for overall water splitting, Nano Research, 14 (2021) 3474-3481.

[2] J. Ren, H. Zong, Y. Sun, S. Gong, Y. Feng, Z. Wang, L. Hu, K. Yu, Z. Zhu, 2D organ-like molybdenum carbide (MXene) coupled with MoS 2 nanoflowers enhances the catalytic activity in the hydrogen evolution reaction, CrystEngComm, 22 (2020) 1395-1403.

[3] K.R.G. Lim, A.D. Handoko, L.R. Johnson, X. Meng, M. Lin, G.S. Subramanian, B. Anasori, Y. Gogotsi, A. Vojvodic, Z.W. Seh, 2h-Mos2 on Mo2ct X Mxene Nanohybrid for Efficient and Durable Electrocatalytic Hydrogen Evolution, ACS nano, 14 (2020) 16140-16155.

[4] D. Guo, X. Li, Y. Jiao, H. Yan, A. Wu, G. Yang, Y. Wang, C. Tian, H. Fu, A dual-active Co-CoO heterojunction coupled with Ti3C2-MXene for highly-performance overall water splitting, Nano Research, 15 (2022) 238-247.

[5] L.-H. Zheng, C.-K. Tang, Q.-F. Lü, J. Wu, MoS2/Mo2TiC2Tx supported Pd nanoparticles as an efficient electrocatalyst for hydrogen evolution reaction in both acidic and alkaline media, International Journal of Hydrogen Energy, 47 (2022) 11739-11749.

[6] S.A. Zahra, S. Rizwan, MWCNT-modified MXene as cost-effective efficient bifunctional catalyst for overall water splitting, RSC advances, 12 (2022) 8405-8413.

[7] S. Peng, Y. Xie, H. Yu, L. Deng, D. Yu, L. Li, R. Amin, A.E. Fetohi, M.Y. Maximov, K. El-Khatib, Anchoring stable FeS2 nanoparticles on MXene nanosheets via interface engineering for efficient water splitting, Inorganic Chemistry Frontiers, (2022).

[8] D. Geng, X. Zhao, Z. Chen, W. Sun, W. Fu, J. Chen, W. Liu, W. Zhou, K.P. Loh, Direct synthesis of large-area 2D Mo2C on in situ grown graphene, Advanced Materials, 29 (2017) 1700072.

[9] D.A. Kuznetsov, Z. Chen, P.V. Kumar, A. Tsoukalou, A. Kierzkowska, P.M. Abdala, O.V. Safonova, A. Fedorov, C.R. Müller, Single site cobalt substitution in 2D molybdenum carbide (MXene) enhances catalytic activity in the hydrogen evolution reaction, Journal of the American Chemical Society, 141 (2019) 17809-17816.

[10] J. Sun, Z. Huang, T. Huang, X. Wang, X. Wang, P. Yu, C. Zong, F. Dai, D. Sun, Defect-rich porous CoS1. 097/MoS2 hybrid microspheres as electrocatalysts for pH-universal hydrogen evolution, ACS Applied Energy Materials, 2 (2019) 7504-7511.

[11] P.V. Shinde, P. Mane, B. Chakraborty, C.S. Rout, Spinel NiFe2O4 nanoparticles decorated 2D Ti3C2 MXene sheets for efficient water splitting: Experiments and theories, Journal of Colloid and Interface Science, 602 (2021) 232-241.
[12] S. Han, Y. Chen, Y. Hao, Y. Xie, D. Xie, Y. Chen, Y. Xiong, Z. He, F. Hu, L. Li, Multi-dimensional hierarchical CoS2@ MXene as trifunctional electrocatalysts for zinc-air batteries and overall water splitting, Science China Materials, 64 (2021) 1127-1138.
[13] L. Fang, W. Li, Y. Guan, Y. Feng, H. Zhang, S. Wang, Y. Wang, Tuning unique peapod-like Co (SxSe1–x) 2 nanoparticles for efficient overall water splitting, Advanced Functional Materials, 27 (2017) 1701008.
[14] C.F. Du, K.N. Dinh, Q. Liang, Y. Zheng, Y. Luo, J. Zhang, Q. Yan, Self-assemble and in situ formation of Ni1− xFexPS3 nanomosaic-decorated MXene hybrids for overall water splitting, Advanced Energy Materials, 8 (2018) 1801127.
[15] N.C.S. Selvam, J. Lee, G.H. Choi, M.J. Oh, S. Xu, B. Lim, P.J. Yoo, MXene supported Co x A y (A= OH, P, Se) electrocatalysts for overall water splitting: unveiling the role of anions in intrinsic activity and stability, Journal of Materials Chemistry A, 7 (2019) 27383-27393.
[16] J. Ding, S. Ji, H. Wang, H. Gai, F. Liu, V. Linkov, R. Wang, Mesoporous nickel-sulfide/nickel/N-doped carbon as HER and OER bifunctional electrocatalyst for water electrolysis, International Journal of Hydrogen Energy, 44 (2019) 2832-2840.
[17] S. Sun, Z. Wang, S. Meng, R. Yu, D. Jiang, M. Chen, Iron and chromium co-doped cobalt phosphide porous nanosheets as robust bifunctional electrocatalyst for efficient water splitting, Nanotechnology, 33 (2021) 075204.
[18] B. Lu, J. Zang, W. Li, J. Li, Q. Zou, Y. Zhou, Y. Wang, Co-doped NixPy loading on Co3O4 embedded in Ni foam as a hierarchically porous self-supported electrode for overall water splitting, Chemical Engineering Journal, 422 (2021) 130062.
[19] X. Peng, S. Zhao, Y. Mi, L. Han, X. Liu, D. Qi, J. Sun, Y. Liu, H. Bao, L. Zhuo, Trifunctional single-atomic Ru sites enable efficient overall water splitting and oxygen reduction in acidic media, Small, 16 (2020) 2002888.
[20] L. Zhang, Z. Wang, W. Chen, R. Yuan, K. Zhan, M. Zhu, J. Yang, B. Zhao, Fe 3 O 4 nanoplates anchored on Ti 3 C 2 T x MXene with enhanced pseudocapacitive and electrocatalytic properties, Nanoscale, 13 (2021) 15343-15351.
[21] Y. Lu, D. Fan, Z. Chen, W. Xiao, C. Cao, X. Yang, Anchoring Co3O4 nanoparticles on MXene for efficient electrocatalytic oxygen evolution, Science Bulletin, 65 (2020) 460-466.

[22] H. Zou, B. He, P. Kuang, J. Yu, K. Fan, Metal–organic framework-derived nickel–cobalt sulfide on ultrathin mxene nanosheets for electrocatalytic oxygen evolution, ACS applied materials & interfaces, 10 (2018) 22311-22319.
[23] T.A. Le, N.Q. Tran, Y. Hong, M. Kim, H. Lee, Porosity-Engineering of MXene as a Support Material for a Highly Efficient Electrocatalyst toward Overall Water Splitting, ChemSusChem, 13 (2020) 945-955.